Science Translational Medicine
AAAS

stm.sciencemag.org/cgi/content/full/12/553/eaay1063/DC1

Supplementary Materials for

siRNA nanoparticles targeting CaMKIIγ in lesional macrophages improve atherosclerotic plaque stability in mice

Wei Tao, Arif Yurdagul Jr., Na Kong, Wenliang Li, Xiaobo Wang, Amanda C. Doran, Chan Feng, Junqing Wang, Mohammad Ariful Islam, Omid C. Farokhzad*, Ira Tabas*, Jinjun Shi*

*Corresponding author. Email: ofarokhzad@bwh.harvard.edu (O.C.F.); iat1@columbia.edu (I.T.); jshi@bwh.harvard.edu (J.S.)

Published 22 July 2020, *Sci. Transl. Med.* **12**, eaay1063 (2020)
DOI: 10.1126/scitranslmed.aay1063

This PDF file includes:

Fig. S1. Synthesis of DSPE-PEG-S2P and its characterization by ^{1}H NMR spectrum.
Fig. S2. Assessment of NP stability.
Fig. S3. Change of NP diameter over time.
Fig. S4. Encapsulation efficiency of siRNA in $S2P_0$ and $S2P_{50}$ NPs.
Fig. S5. NP morphology.
Fig. S6. Serum stability of siRNA-loaded $S2P_{50}$ NPs.
Fig. S7. Silencing of luciferase in HeLa-Luc cells by $S2P_0$-siLuc NPs.
Fig. S8. Effect of $S2P_{50}$-siLuc NPs on cell viability in vitro.
Fig. S9. Apoptosis assays.
Fig. S10. Proliferation assays.
Fig. S11. NP uptake and stabilin-2 expression in macrophages and nonmacrophage cell types.
Fig. S12. Time course of Dy647 fluorescence in whole blood of mice injected with free Dy647-siRNA or Dy647-siRNA in $S2P_0$ and $S2P_{50}$ NPs.
Fig. S13. Gating strategy for aortic macrophages.
Fig. S14. Biodistribution of Alexa 647–conjugated $S2P_0$- and $S2P_{50}$-siCamk2g NPs.
Fig. S15. FACS analysis of fluorescent NPs in splenocytes 24 hours after NP injection into WD-fed *Ldlr*$^{-/-}$ mice.
Fig. S16. Effect of siCamk2g $S2P_{50}$ NPs on macrophage efferocytosis.
Fig. S17. CaMKIIγ silencing with NPs enhances efferocytosis as assessed by flow cytometry.
Fig. S18. CaMKIIγ expression in lesional SMCs and ECs in NP-treated *Ldlr*$^{-/-}$ mice.
Fig. S19. CaMKIIγ expression in splenic macrophages in NP-treated *Ldlr*$^{-/-}$ mice.
Fig. S20. CaMKIIγ expression in liver macrophages in NP-treated *Ldlr*$^{-/-}$ mice.
Fig. S21. Metabolic parameters and blood cell counts of WD-fed *Ldlr*$^{-/-}$ mice treated with PBS or $S2P_{50}$ NPs containing control siRNA or siCamk2g.
Fig. S22. Histological analyses of the major organs in NP-treated *Ldlr*$^{-/-}$ mice.

Fig. S23. Plasma TNF-α and IL-12 concentrations in mice injected with PBS, empty $S2P_{50}$ NPs, or $S2P_{50}$-siCamk2g NPs.
Fig. S24. Summary scheme of the study.

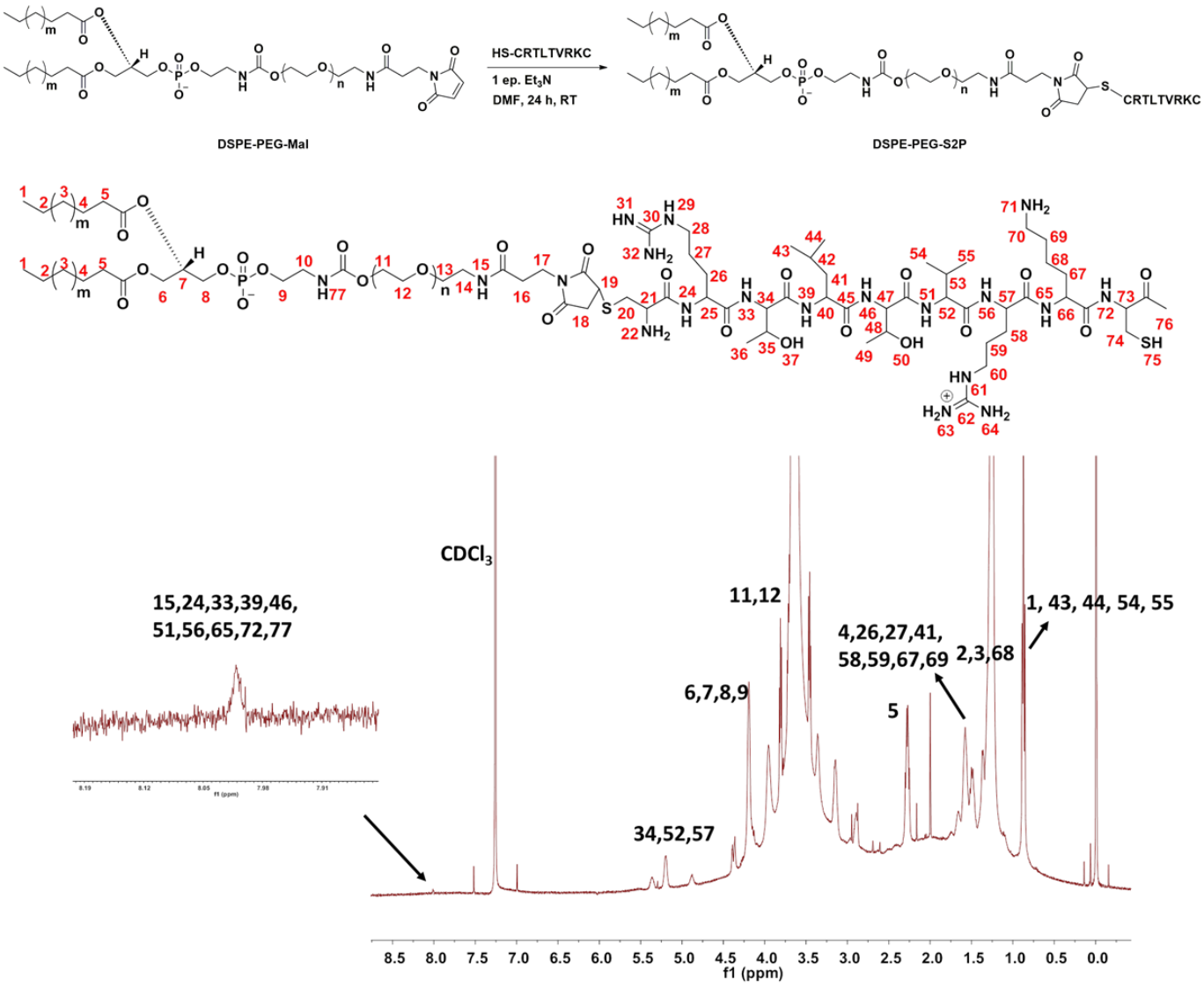

Fig. S1. Synthesis of DSPE-PEG-S2P and its characterization by ^{1}H NMR spectrum. See Materials and Methods for synthesis protocol. The numbers in red on the structure correspond to the peaks on the ^{1}H NMR spectrum.

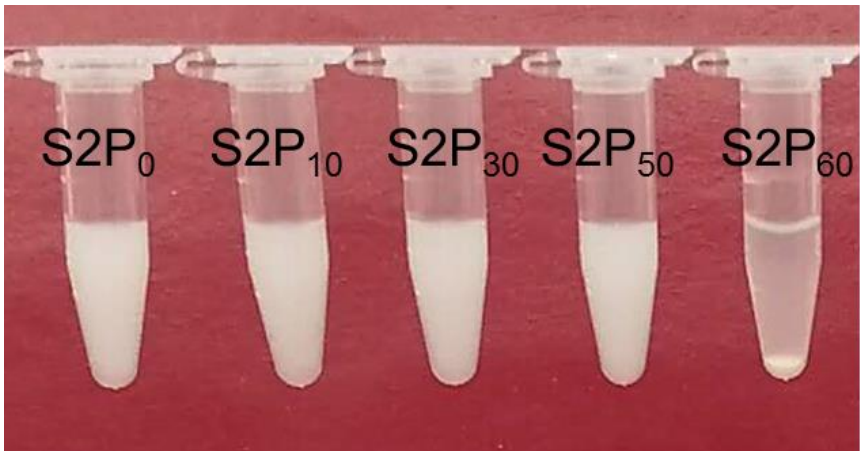

Fig. S2. Assessment of NP stability. NPs without S2P or with the indicated percentages of S2P were incubated with PBS containing 10% serum and then subjected to 24 hours of rotation at 37°C at 100 rpm. Shown are images of the NP suspensions for the NP formulations.

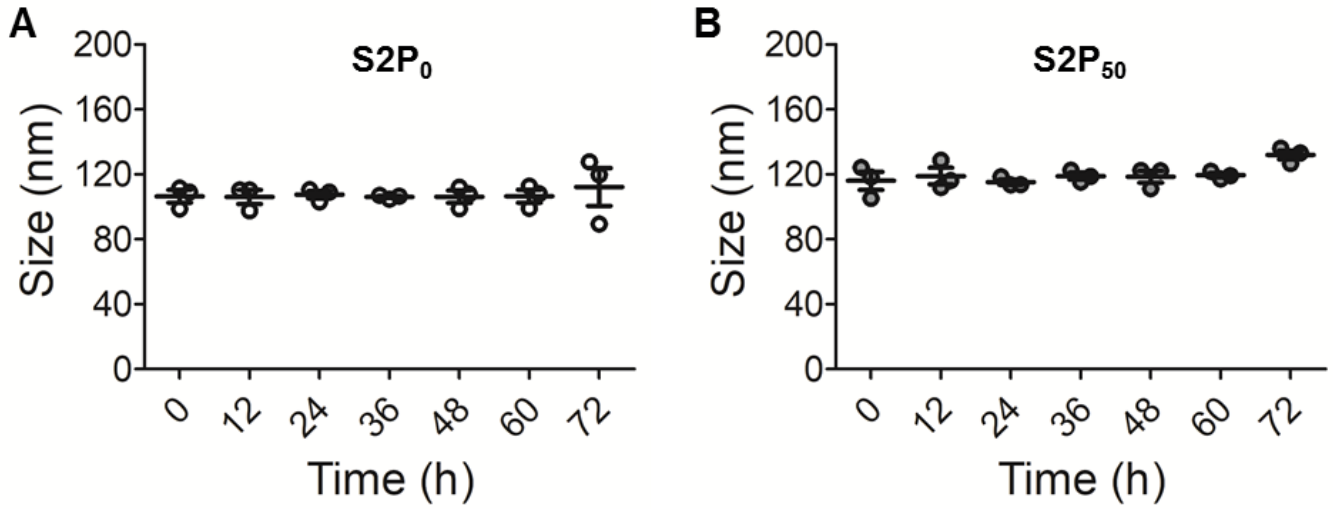

Fig. S3. Change of NP diameter over time. Stability of the non-targeted $S2P_0$ and targeted $S2P_{50}$ NPs over 3 days in PBS containing 10% serum at 37°C. The diameters of the fresh prepared NPs after different hours of incubation were determined by dynamic light scattering (DLS) measurements.

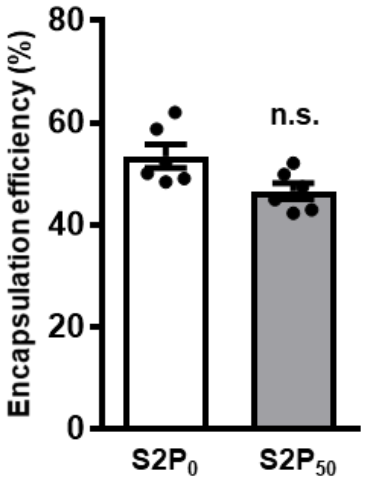

Fig. S4. Encapsulation efficiency of siRNA in $S2P_0$ and $S2P_{50}$ NPs. Non-targeted NPs ($S2P_0$) and targeted S2P-NPs ($S2P_{50}$) NPs were loaded with Dy647-labeled siRNA. The purified NPs were then extracted with DMSO, followed by quantification of the extracted Dy647 fluorescence. Encapsulated efficiency (EE) is defined as the fraction of fluorescent siRNA added during the NP construction procedure that that was extracted from the purified NPs (*n* = 6 preparations of NPs per group, mean ± SEM). Statistical significance was determined using Student's *t* test. (*n.s.*, not significant).

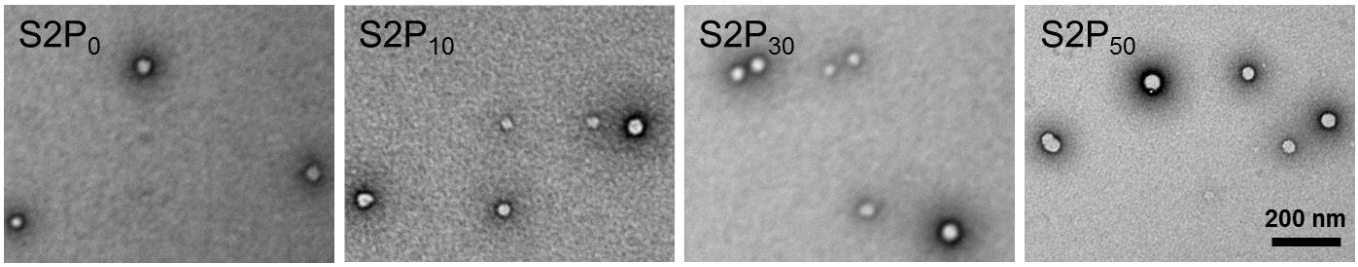

Fig. S5. NP morphology. Transmission electron microscopic (TEM) images of siRNA-loaded NPs at different densities of S2P. From left to right: $S2P_0$, $S2P_{10}$, $S2P_{30}$, and $S2P_{50}$ NPs.

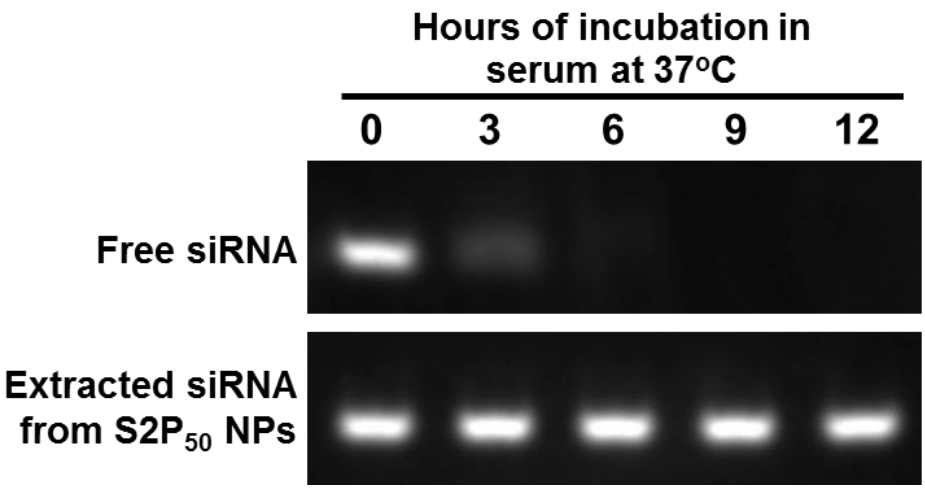

Fig. S6. Serum stability of siRNA-loaded $S2P_{50}$ NPs. Agarose gel electrophoresis of free siRNA and siRNA extracted from $S2P_{50}$ NPs after incubation in serum at 37°C for 3, 6, 9, and 12 hours.

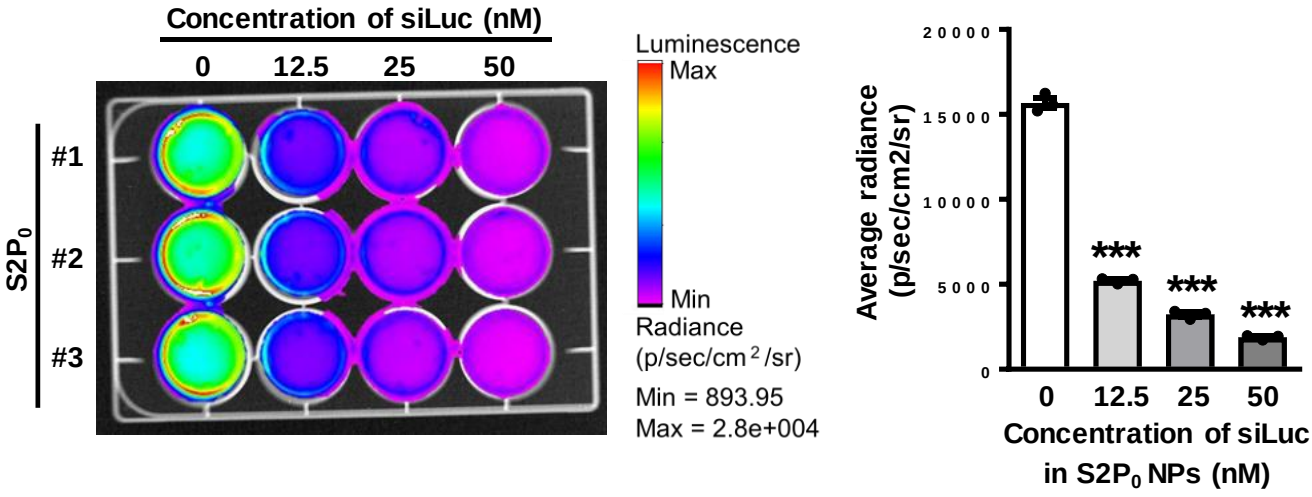

Fig. S7. Silencing of luciferase in HeLa-Luc cells by $S2P_0$-siLuc NPs. Bioluminescence imaging of luciferase-expressing HeLa (HeLa-Luc) cells after 24 hours of treatment with $S2P_0$ NPs loaded with the indicated concentrations of siLuc. The graph shows the average radiance of the cells (n = 3 plates of cell per group, mean ± SEM). Statistical significance was determined using one-way ANOVA (***P < 0.001).

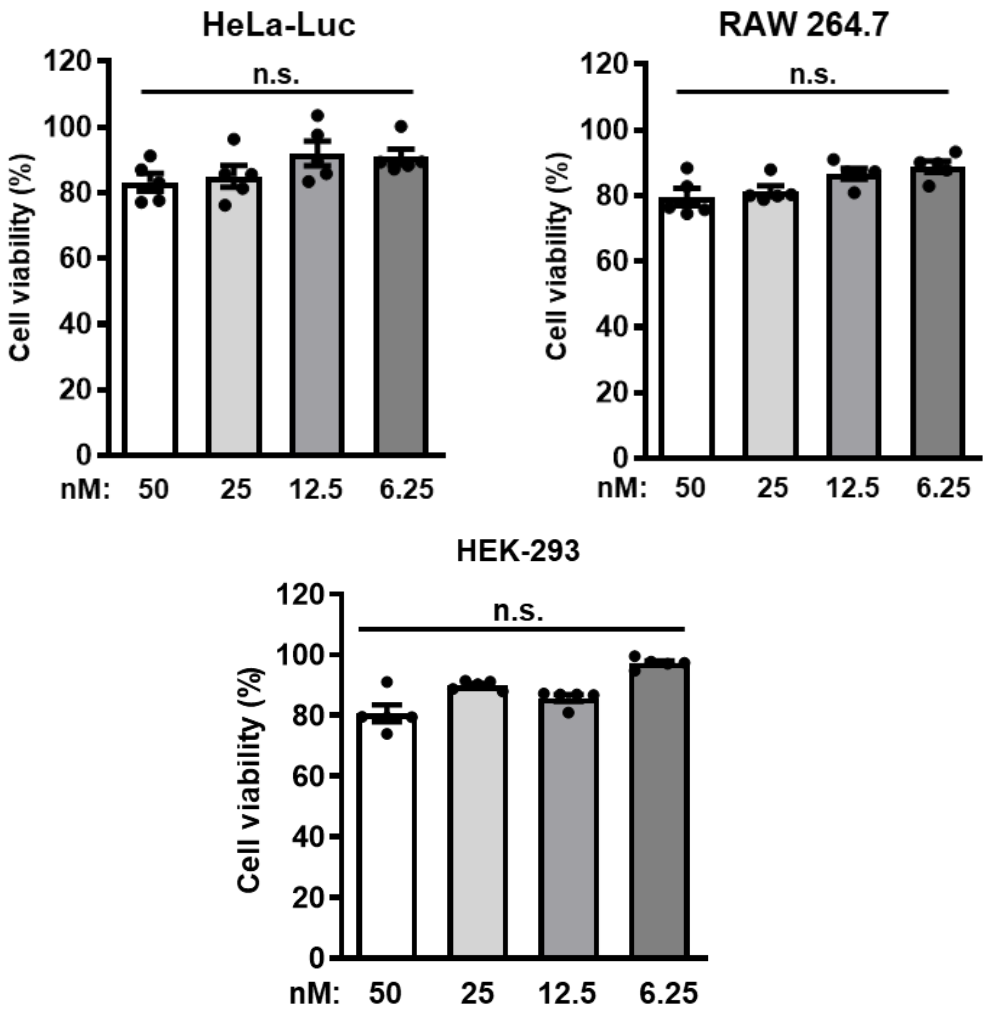

Fig. S8. Effect of $S2P_{50}$-siLuc NPs on cell viability in vitro. Hela-Luc, RAW 264.7, and HEK-293 cells were incubated for 24 hours with the indicated concentrations of $S2P_{50}$ NPs based on nM of siLuc content, and after an addition 48 hours of incubation, the cells were assayed for viability using the alamarBlue cell viability reagent (n = 5 plates of cells per group, mean ± SEM). Statistical significance was determined using one-way ANOVA (*n.s.*, not significant).

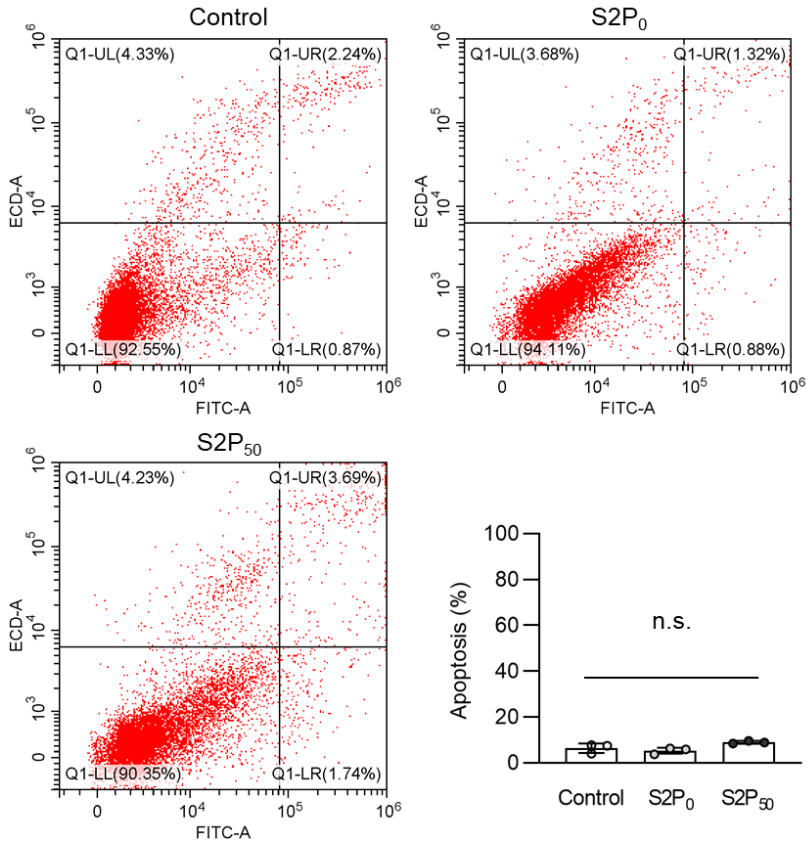

Fig. S9. Apoptosis assays. RAW 264.7 macrophage cells were incubated for 24 hours with non-targeted $S2P_0$ NPs or targeted $S2P_{50}$ NPs at the siRNA concentration of 50 nM, or same-volume PBS control, and after an additional 48 hours of incubation, the cells were assayed for apoptosis using flow cytometry (n = 3, mean ± SEM). Statistical significance was determined using one-way ANOVA (n.s., not significant).

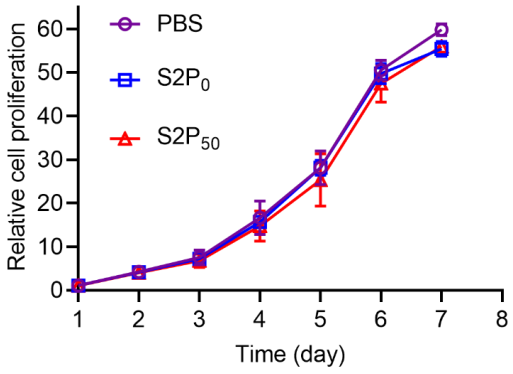

Fig. S10. Proliferation assays. RAW 264.7 macrophage cells were incubated for 24 hours with non-targeted $S2P_0$ NPs or targeted $S2P_{50}$ NPs at an siRNA concentration of 50 nM, or same-volume PBS control, on day 0. After the treatment, the NP effect on the cell proliferation was monitored over 7 days.

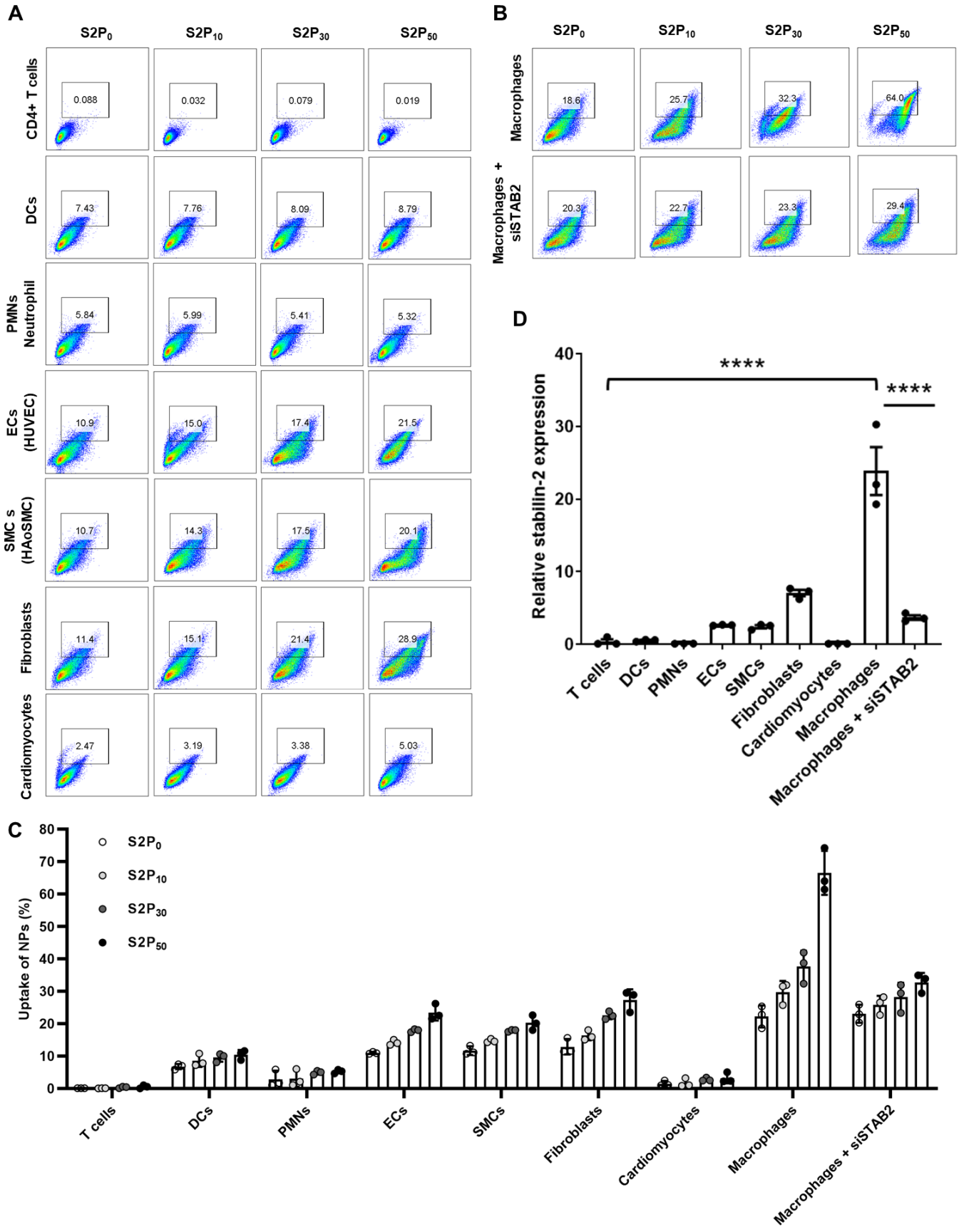
A
S2P0
S2P10
S2P30
S2P50
CD4+ T cells
0.088
0.032
0.079
0.019
DCs
7.43
7.76
8.09
8.79
PMNs Neutrophil
5.84
5.99
5.41
5.32
ECs (HUVEC)
10.9
15.0
17.4
21.5
SMC s (HAoSMC)
10.7
14.3
17.5
20.1
Fibroblasts
11.4
15.1
21.4
28.9
Cardiomyocytes
2.47
3.19
3.38
5.03
B
Macrophages
18.6
25.7
32.3
64.0
Macrophages + siSTAB2
20.3
22.7
23.3
29.4
D
Relative stabilin-2 expression
****
****
T cells
DCs
PMNs
ECs
SMCs
Fibroblasts
Cardiomyocytes
Macrophages
Macrophages + siSTAB2
C
Uptake of NPs (%)
S2P0
S2P10
S2P30
S2P50
T cells
DCs
PMNs
ECs
SMCs
Fibroblasts
Cardiomyocytes
Macrophages
Macrophages + siSTAB2

Fig. S11. NP uptake and stabilin-2 expression in macrophages and nonmacrophage cell types. (**A**) Human CD4+ T cells, human dendritic cells (DCs), human polymorphonuclear cells (PMNs), human umbilical vein endothelial cells (ECs), human aortic smooth muscle cells (SMCs), human fibroblasts, and human cardiomyocytes were incubated for 2 hours with Dy647-labeled NPs with the indicated S2P density and with an siRNA concentration of 50 nM. The percent uptake of labeled NPs was quantified by flow cytometry. (**B**) The uptake of NPs in mouse macrophages transfected with stabilin-2 siRNA (siSTAB2) was tested under the same conditions using flow cytometry. (**C**) Quantified NP uptake data as assayed by flow cytometry (n = 3). (**D**) Relative *STAB2* mRNA expression in the different cell types.

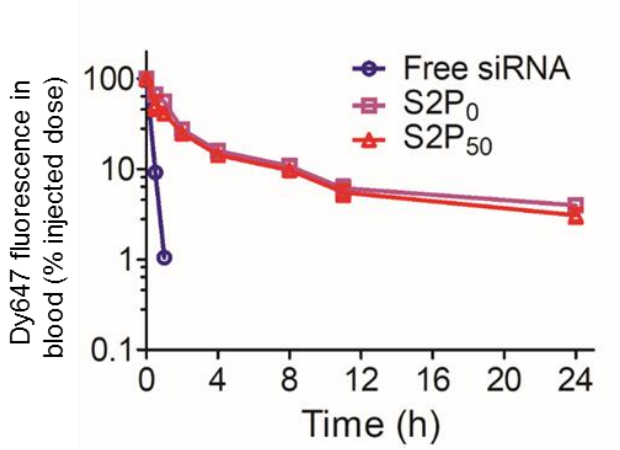

Fig. S12. Time course of Dy647 fluorescence in whole blood of mice injected with free Dy647-siRNA or Dy647-siRNA in $S2P_0$ and $S2P_{50}$ NPs. BALB/c mice were injected intravenously with free Dy647-siRNA or Dy647-siRNA loaded in $S2P_0$ or $S2P_{50}$ NPs at the siRNA dose of 1 nmol per mouse. After the indicated times, blood was assayed for fluorescence intensity of Dy647. Data shown are percent of injected fluorescence (*n* = 3 mice per group, mean ± SEM).

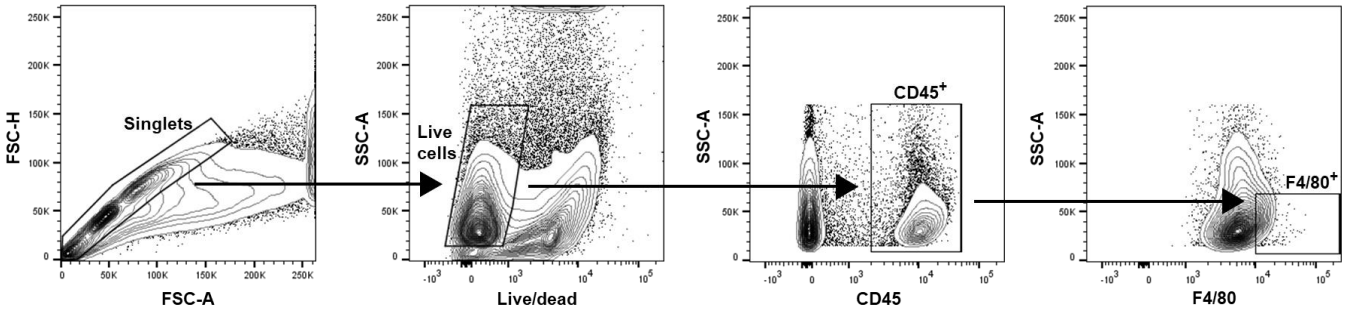

Fig. S13. Gating strategy for aortic macrophages. Aortic cells were stained with an Aqua Live/Dead cell dye and immunostained for CD45 and F4/80. Cells were then gated on single cell populations (FSC-H/FSC-A), live cells ($Aqua^-$), $CD45^+$ cells, and $F4/80^+$ cells.

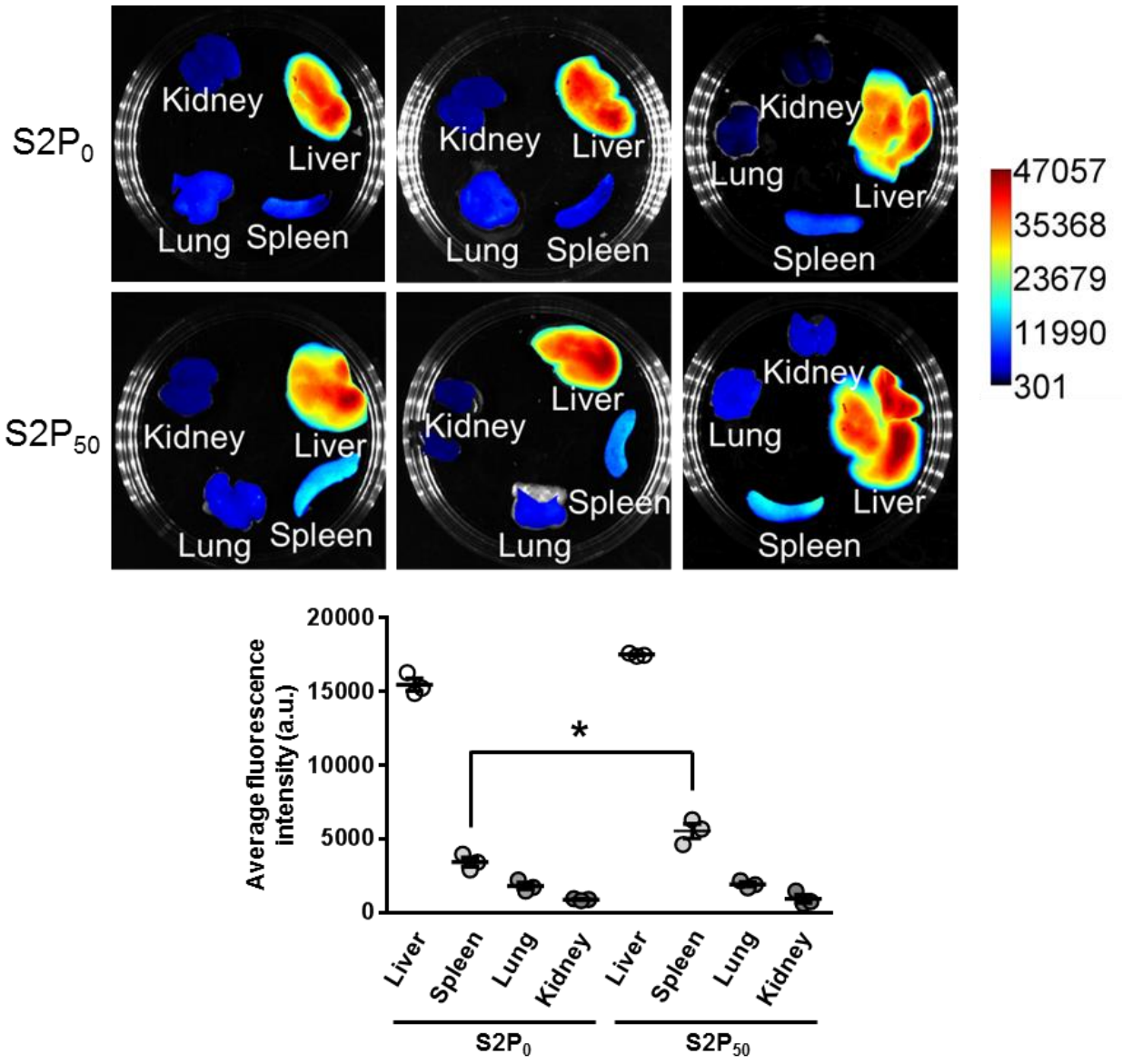

Fig. S14. Biodistribution of Alexa 647–conjugated $S2P_0$- and $S2P_{50}$-siCamk2g NPs. 12-wk-WD-fed *Ldlr*$^{-/-}$ mice were injected intravenously with PBS, non-targeted Alexa 647-conjugated $S2P_0$-siCamk2g NPs, or Alexa 647-conjugated $S2P_{50}$-siCamk2g NPs at the dose of 1 nmol of siRNA per mouse. The mice received another injection 24 hours later. Twenty-four hours after the second injection, the mice were euthanized, and the indicated organs were imaged using a CRi Maestro II In-Vivo Imaging System. The imaging date were quantified using ImageJ (n = 3 mice per group, mean ± SEM). Statistical significance was determined using Student's t test. *P < 0.05 for $S2P_0$ versus $S2P_{50}$ spleen groups.

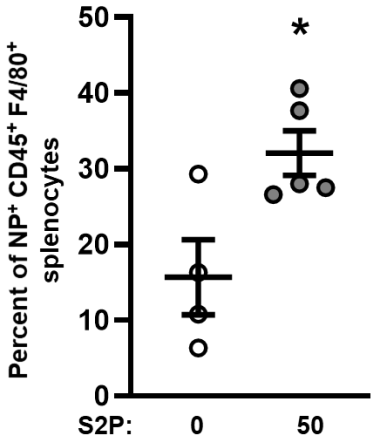

Fig. S15. FACS analysis of fluorescent NPs in splenocytes 24 hours after NP injection into WD-fed *Ldlr*$^{-/-}$ mice. 8-week WD-fed *Ldlr*$^{-/-}$ were injected once intravenously with $S2P_0$ AF647-NPs, or $S2P_{50}$ AF647-NPs. Spleens were harvested 24 hrs later, and splenic cells were isolated and immunostained for CD45 and F4/80 followed by flow cytometry analysis (n = 4-5 mice per group, mean + SEM). Statistical significance was determined using Student's *t* test. **P* < 0.05.

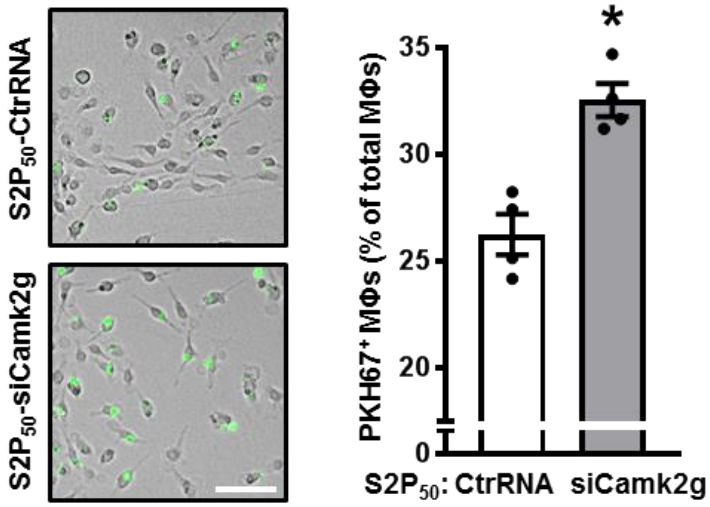

Fig. S16. Effect of siCamk2g $S2P_{50}$ NPs on macrophage efferocytosis. Bone marrow-derived macrophages (BMDMs) were treated with $S2P_{50}$ NPs containing 50 nM of either control RNA (CtrRNA) or siCamk2g. Three days later, PKH67-labelled apoptotic cells were added at a 3:1 apoptotic cell:macrophage ratio. After 45 minutes, unbound apoptotic cells were removed, and the percent of apoptotic cells engulfed by the macrophages was quantified by fluorescence microscopy (*n* = 4 plates of macrophages for each group). Scale bar, 40 μm. Error bars represent SEM. Statistical significance was determined using Student's *t* test. **P* < 0.05.

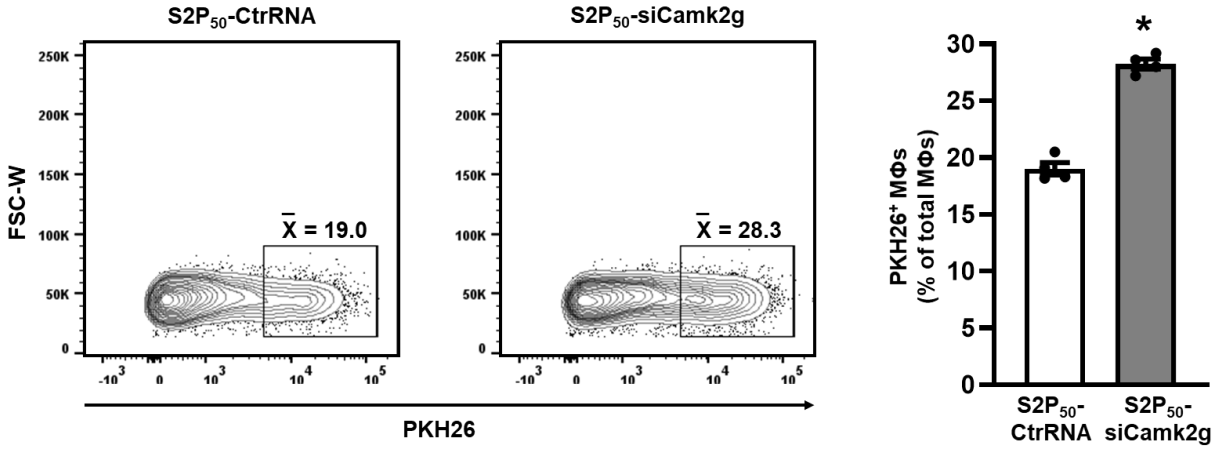

Fig. S17. CaMKIIγ silencing with NPs enhances efferocytosis as assessed by flow cytometry. Bone marrow-derived macrophages (BMDMs) were treated with $S2P_{50}$ NPs containing 50 nM of either scrambled RNA (ScrRNA) or siCamk2g. Three days later, PKH26-labeled apoptotic cells were added at a 3:1 apoptotic cell:macrophage ratio. After 45 minutes, unbound apoptotic cells were removed, and the percent of apoptotic cells engulfed by the macrophages was quantified by flow cytometry (n = 4 plates of macrophages for each group). Statistical significance was determined using Student's *t* test. **P* < 0.05.

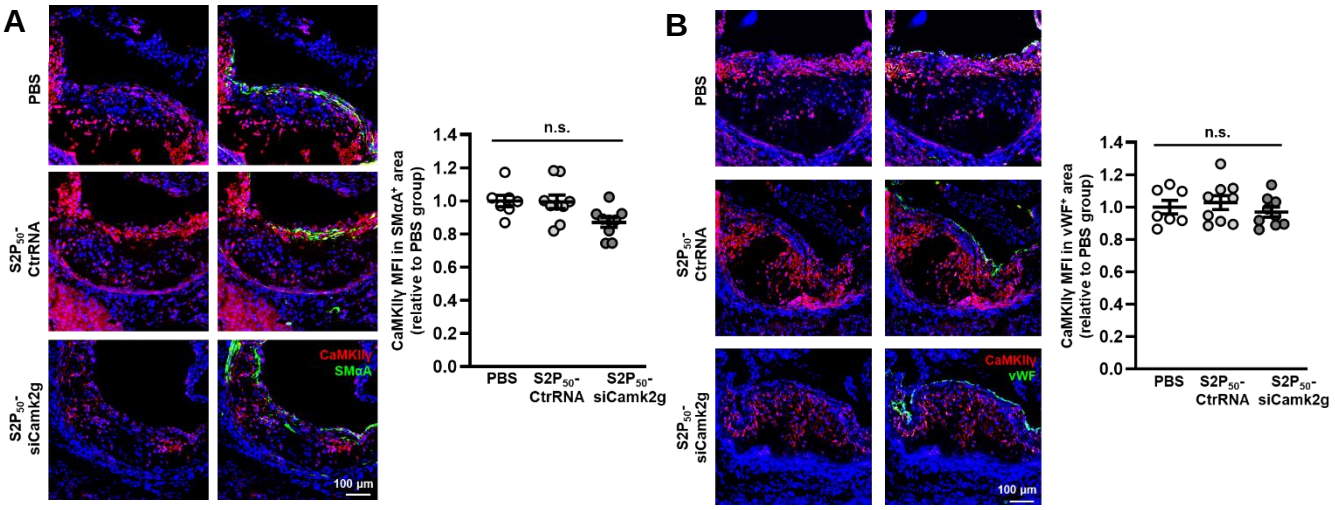

Fig. S18. CaMKIIγ expression in lesional SMCs and ECs in NP-treated *Ldlr*$^{-/-}$ mice. 8-week WD-fed *Ldlr*$^{-/-}$ were injected intravenously twice a week for 4 weeks with PBS, $S2P_{50}$ NPs loaded with CtrRNA (1 nmol of CtrRNA per injection), or $S2P_{50}$ NPs carrying siCamk2g (1 nmol of siCamk2g per injection while being maintained on the WD. Cross-sections of aortic roots were immunostained for CaMKIIγ, SMαA, or vWF, then counterstained with DAPI. The staining data were quantified as MFI of CaMKIIγ in the SMαA$^+$ area (**A**) or vWF$^+$ area (**B**) relative to PBS group (*n* = 7-9 mice per group).

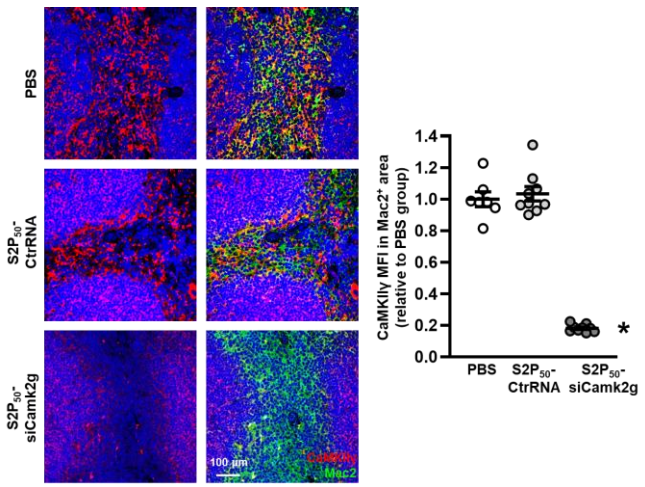

Fig. S19. CaMKIIγ expression in splenic macrophages in NP-treated *Ldlr*$^{-/-}$ mice. 8-week WD-fed *Ldlr*$^{-/-}$ were injected intravenously twice a week for 4 weeks with PBS, $S2P_{50}$ NPs loaded with CtrRNA (1 nmol of CtrRNA per injection), or $S2P_{50}$ NPs carrying siCamk2g (1 nmol of siCamk2g per injection) while being maintained on the WD. Cross-sections of spleens were immunostained for CaMKIIγ and Mac2 then counterstained with DAPI. The staining data were quantified as MFI of CaMKIIγ in the Mac2^{+} area relative to PBS group (*n* = 7-9 mice per group, mean +SEM). Data were normal and statistical significance was determined using one-way ANOVA. *P < 0.05 versus the other two groups.

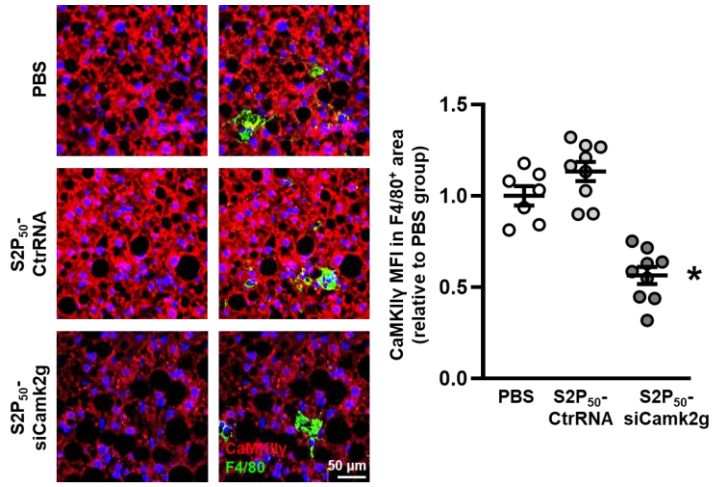

Fig. S20. CaMKIIγ expression in liver macrophages in NP-treated *Ldlr*$^{-/-}$ mice. 8-week WD-fed *Ldlr*$^{-/-}$ were injected intravenously twice a week for 4 weeks with PBS, $S2P_{50}$ NPs loaded with CtrRNA (1 nmol of CtrRNA per injection), or $S2P_{50}$ NPs carrying siCamk2g (1 nmol of siCamk2g per injection) while being maintained on the WD. Cross-sections of livers were immunostained for CaMKIIγ and F4/80 then counterstained with DAPI. The staining data were quantified as MFI of CaMKIIγ in the F4/80^{+} area relative to PBS group (*n* = 7-9 mice per group, mean +SEM). Data were normal and statistical significance was determined using one-way ANOVA. *P < 0.05 versus the other two groups.

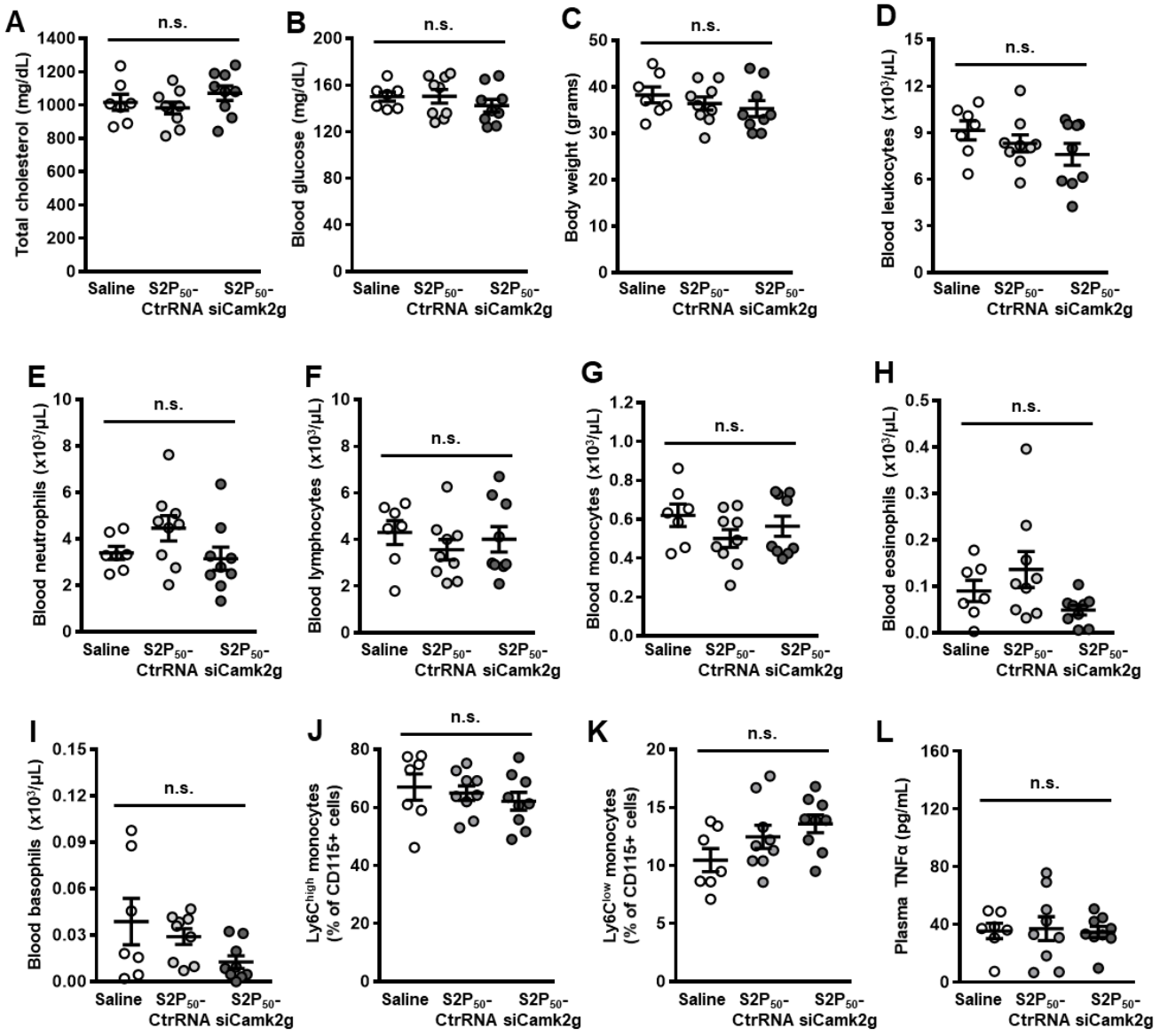

Fig. S21. Metabolic parameters and blood cell counts of WD-fed *Ldlr*$^{-/-}$ mice treated with PBS or S2P$_{50}$ NPs containing control siRNA or siCamk2g. (**A**) Plasma cholesterol, (**B**) fasting blood glucose, (**C**) body weight, (**D-I**) complete blood counts, (**J**) circulating Ly6C^{high} and (**K**) Ly6C^{low} monocytes profiles, and (**L**) plasma TNFα concentration from the mice described in Figure 4. All data except for H fit a normal distribution. The data in panels A-G and I-L were analyzed by one-way ANOVA, and the data in panel H were analyzed by the Kruskal-Wallis test. Error bars represent SEM (*n* = 7-9 mice per group). *n.s.*, not significant.

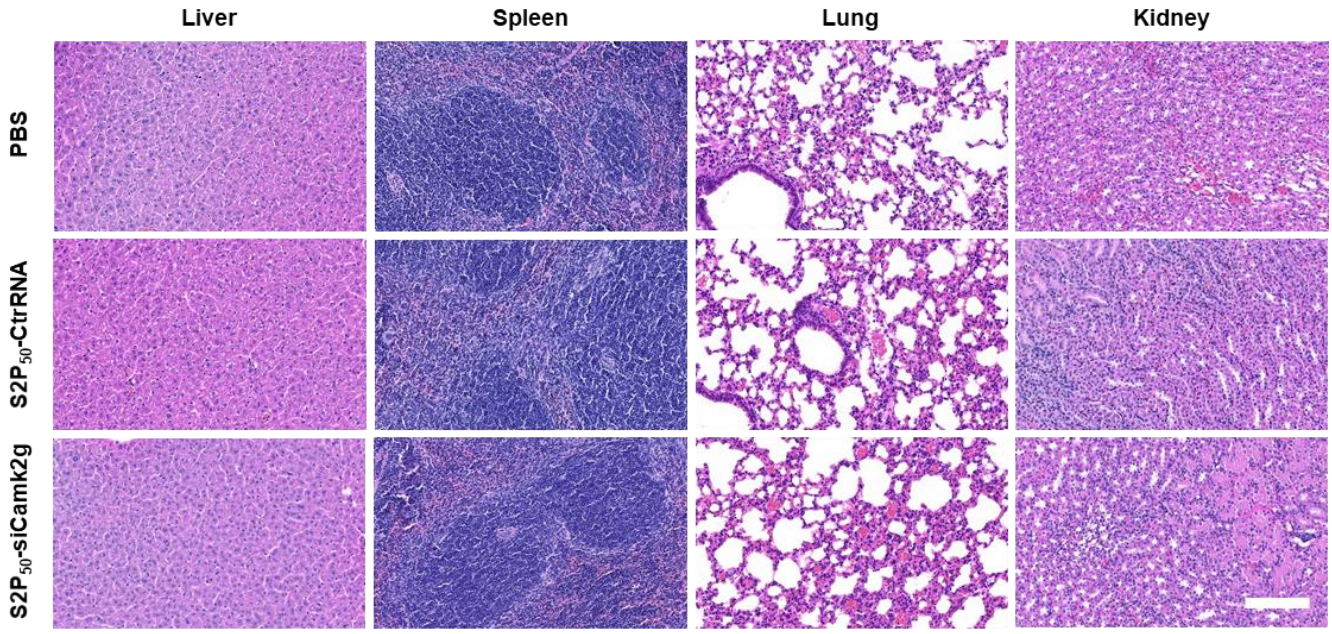

Fig. S22. Histological analyses of the major organs in NP-treated *Ldlr*$^{-/-}$ mice. 8-week WD-fed *Ldlr*$^{-/-}$ were injected intravenously twice a week for 4 weeks with PBS, S2P$_{50}$ NPs loaded with CtrRNA (1 nmol of CtrRNA per injection), or S2P$_{50}$ NPs carrying siCamk2g (1 nmol of siCamk2g per injection while being maintained on the WD. Three days after the last injection, the mice were euthanized, and the indicated organs were sectioned and stained with H&E. Scale bar, 100 μm.

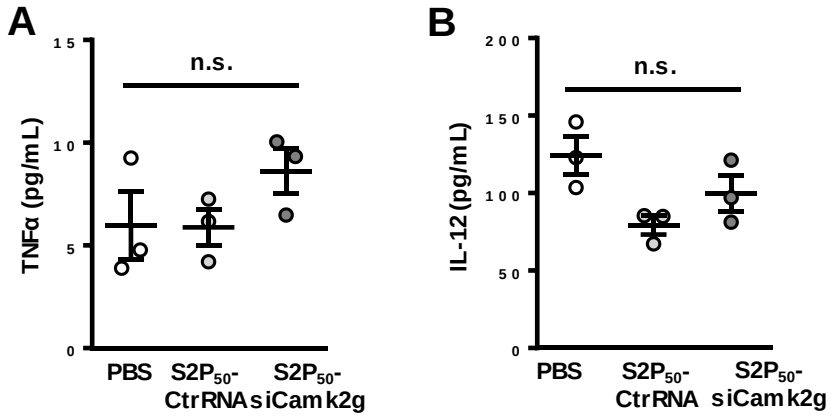

Fig. S23. Plasma TNF-α and IL-12 concentrations in mice injected with PBS, empty S2P$_{50}$ NPs, or S2P$_{50}$-siCamk2g NPs. Female BALB/c mice were injected intravenously with PBS, empty S2P$_{50}$ NPs, or S2P$_{50}$-siCamk2g NPs at an siRNA dose of 1 nmol per mouse. The empty S2P$_{50}$ NPs were injected at the same NP dose as the S2P$_{50}$-siCamk2g NPs. Twenty-four hours later, serum samples were analyzed by ELISA for (**A**) TNF-α and (**B**) IL-12. Error bars represent SEM (n = 3). Statistical significance was determined using one-way ANOVA (*n.s.*, not significant).

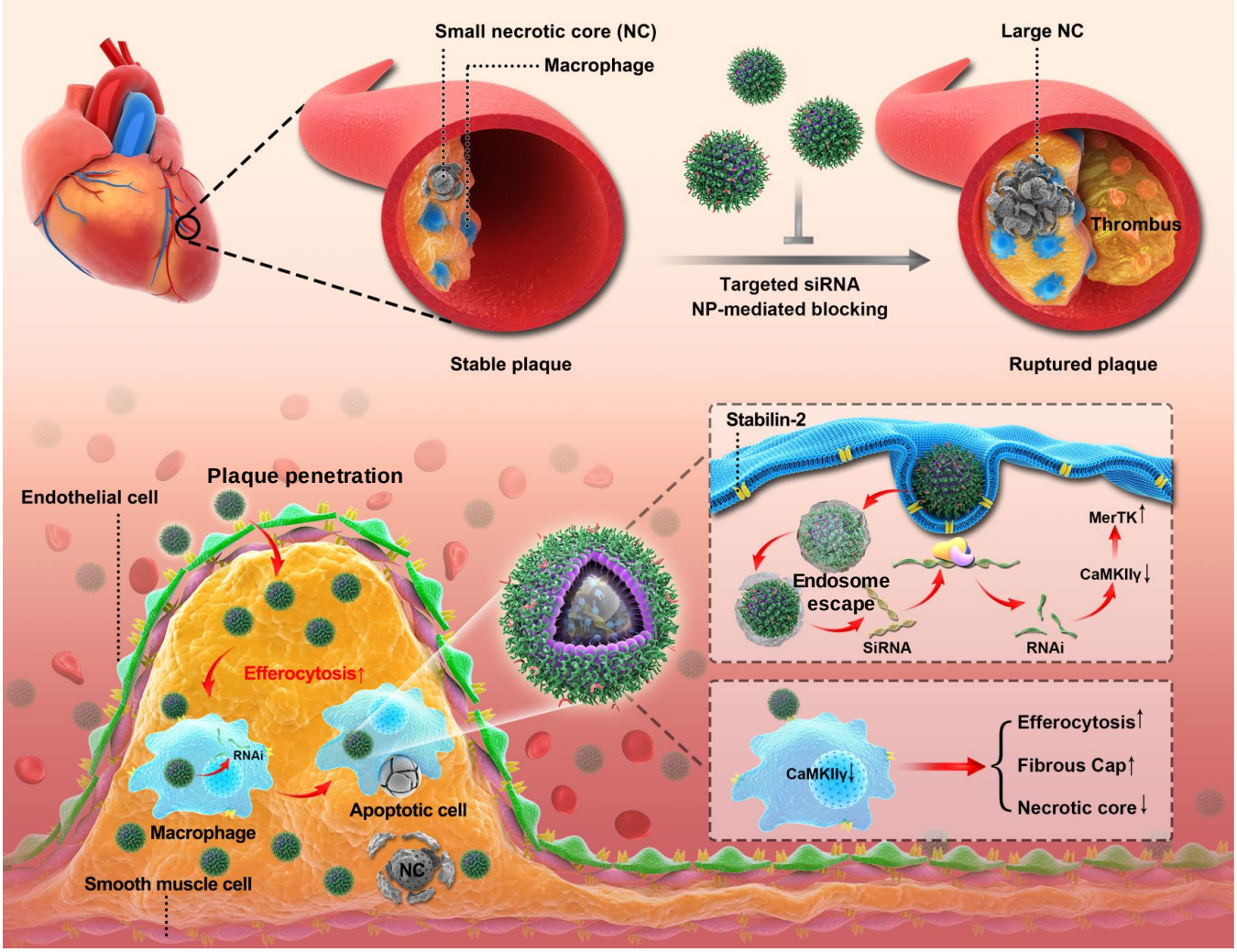

Fig. S24. Summary scheme of the study. The upper scheme demonstrates the overall principle of using macrophage-targeted siRNA-containing NPs to block the progression of stable atherosclerotic lesions to the type of necrotic plaques that can rupture and precipitate vaso-occlusive thrombosis. The bottom scheme summarizes the major findings of this study using $S2P_{50}$-siCamk2g NPs. The NPs enter atherosclerotic lesions, get taken up by lesional macrophages, escape endosomes to release their siRNA, and silence plaque-destabilizing CaMKIIγ. Through mechanisms described previously, silencing of CaMKIIγ increases MerTK-mediated efferocytosis, leading to decreased plaque necrosis and more stable fibrous caps. These findings demonstrate that atherosclerosis-promoting genes in plaque macrophages can be targeted with siRNA NPs and demonstrate the application of this strategy in a pre-clinical model of advanced atherosclerosis.